Modelling thermal sensitivity in the full phenological distribution: a new approach applied to the spring arboreal caterpillar peak

Kirsty H. Macphie[1*], Jelmer M. Samplonius[1], Joel L. Pick[1], Jarrod D. Hadfield[1], Albert B. Phillimore[1]

[1] Institute for Ecology and Evolution, The University of Edinburgh, Edinburgh, UK

Corresponding author: K. H. Macphie
Email: kirsty.macphie@ed.ac.uk

Abstract

1. Advances in spring phenology are among the clearest biological responses to climate warming. There has been much interest in how climate impacts on phenology because the timings of key events have implications for species interactions, nutrient cycling and ecosystem services. To date most work has focused on only one aspect of population phenology, the effects of temperature on the average timing. In comparison, effects of temperature on the abundance of individuals and their seasonal spread are understudied, despite their potential to have profound impacts on species interactions.
2. Here we develop a new method that directly estimates the effect of spring temperatures on the timing, height and width of the phenological distribution and apply it to temperate forest caterpillars, a guild that has been the focus of much research on phenology and trophic mismatch.
3. We find that warmer spring conditions advance the timing of the phenological distribution of abundance by -4.96 days $^{o}C^{-1}$ and increase its height by 34% $^{o}C^{-1}$, but have no significant effect on the duration of the distribution. An increase in the maximum density of arboreal caterpillars with rising temperatures has implications for understanding climate impacts on

forest food chains, both in terms of herbivory pressure and the resources available to secondary consumers.

4. The new method we have developed allows the thermal sensitivity in the full phenological distribution to be modelled directly from raw data, providing a flexible approach that has broad applicability within global change research.

Key words: Phenology, thermal sensitivity, trophic match/mismatch, spatiotemporal, caterpillar

Introduction

Anthropogenic climate warming has profound impacts on ecological systems, with phenological shifts having become one of the most reported biotic responses (Walther *et al.* 2002; Parmesan & Yohe 2003). Temperature is a key driver of phenology for extra-tropical taxa, though there is heterogeneity in thermal sensitivity among species and trophic levels (Thackeray *et al.* 2016; Cohen *et al.* 2018; Roslin *et al.* 2021). The outcome of many species interactions depend on synchrony between ephemeral life history events and, as the thermal sensitivity of interacting species or guilds may differ, warming temperatures have the potential to alter interactions, including those between consumers and their resources (Thackeray *et al.* 2016; Kharouba *et al.* 2018; Samplonius *et al.* 2020).

Phenology is frequently quantified as the mean or first timing of an event (Fig. 1a) among individuals in a population (Thomas *et al.* 2001; Charmantier *et al.* 2008; Both *et al.* 2009; Reed *et al.* 2013; Thackeray *et al.* 2016; Burgess *et al.* 2018; Roslin *et al.* 2021) and the thermal sensitivity of mean (or first) timing has been examined for many species and guilds (Thackeray *et al.* 2016; Cohen *et al.* 2018; Roslin *et al.* 2021). In comparison, very few phenology-focused studies have addressed how temperature affects other parameters that determine the full

54 phenological distribution, namely the abundance of individuals exhibiting the mean timing
55 (height), how the timing within a population or guild is spread around the mean (width), or the
56 length of time over which the frequency of a phenological event falls above a given threshold
57 (duration) (Fig 1a). Beyond a phenological context, there is evidence across a range of taxa
58 that temperature affects interannual trends in abundance (Bowler *et al.* 2017). Previous work
59 also finds spatial and temporal trends in the duration of life history events (Vitasse *et al.* 2009;
60 Møller *et al.* 2010; Ahmad *et al.* 2021), although responses vary among species and events.
61 For example, the grasshopper community is abundant for a longer duration in warmer years in
62 Colorado (Buckley *et al.* 2021) and the deciduous tree canopy duration is longer in warmer
63 years in the Pyrenees (Vitasse *et al.* 2009), whilst warmer conditions drive shorter flowering
64 durations for a range of flowing plant species observed on Guernsey (Bock *et al.* 2014) and in
65 Finland more bird species have seen a reduction in the duration of breeding over time than an
66 increase (Hällfors *et al.* 2020).

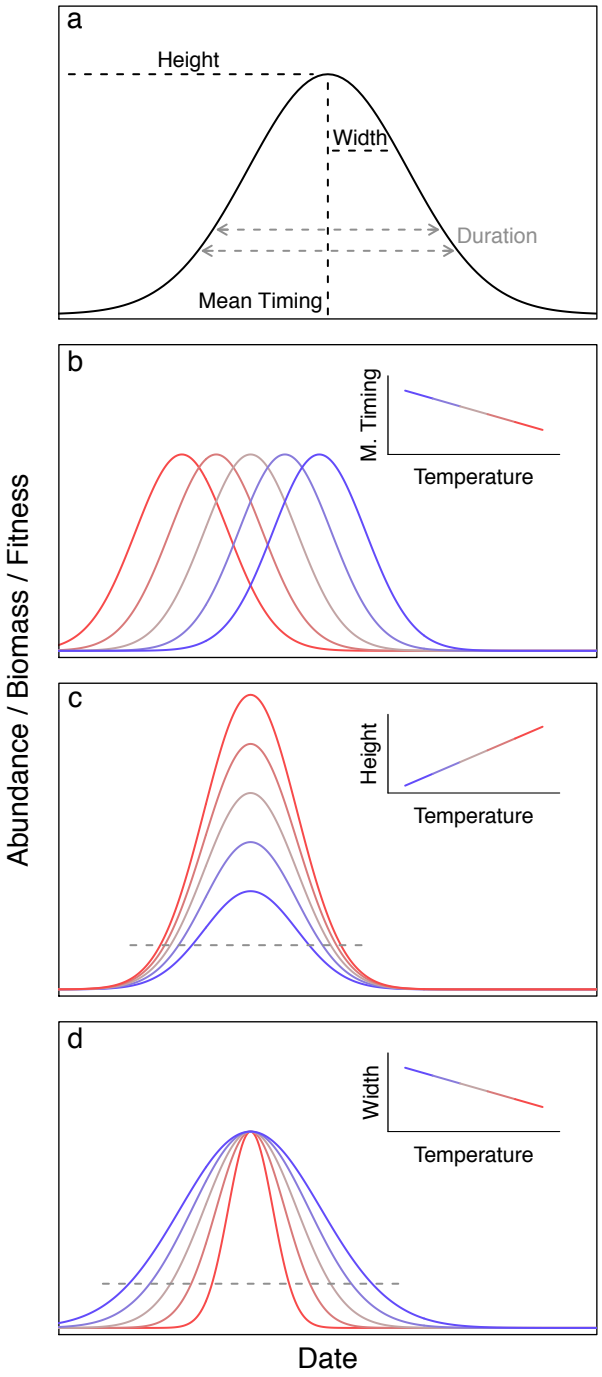

Figure 1: a) a Gaussian function showing the three parameters that govern the phenological distribution (black) of a life history event: mean timing is the most common timing within the population/guild, height describes the maximum response (e.g. abundance, biomass or fitness) value reached, width corresponds to the standard deviation of the function and therefore its curvature. Duration (a derived metric) describes the number of days where the response falls above a given threshold. The chosen threshold level will influence the duration, as illustrated by the two lines. b-d) Examples of how a slope in thermal sensitivity for each parameter could influence the phenological distribution while the other parameters are held constant. The grey dashed lines in c) and d) show that a change in the height or width parameter both influence the duration at a given value and therefore duration is not defined by width alone, as it would be for a Gaussian distribution.

89

90 In the context of research on phenology and the match/mismatch hypothesis (MMH – the
91 hypothesis that phenological asynchrony between consumer demand and an ephemeral
92 resource impacts negatively on consumer fitness (Cushing 1969)), the temperate forest tri-
93 trophic chain of deciduous trees, caterpillars and cavity nesting passerines in spring has become

a classic study system (Thomas *et al.* 2001; Charmantier *et al.* 2008; Both *et al.* 2009; Cole *et al.* 2021). Within this system the phenological distribution of caterpillars may have both top-down and bottom-up effects through interactions with both the leafing trees and breeding birds respectively. The phenological distribution of the caterpillar guild of primary consumers – comprised of many species (Shutt *et al.* 2019) – is usually summarised on the basis of mean timing, which has been found to advance by approximately 4-6 days $^{o}C^{-1}$ (Visser *et al.* 2006; Charmantier *et al.* 2008; Burgess *et al.* 2018); largely tracking the shift in timing of deciduous tree leafing, but a little steeper than the advance of insectivorous passerine breeding (Both *et al.* 2009; Burgess *et al.* 2018; Cole *et al.* 2021). Effects of spring temperature on the height or width of the caterpillar phenological distribution have been largely overlooked. The exceptions are a study that reported no correlation between spring temperature and the height of the caterpillar biomass distribution over 16 years in Poland (Nadolski *et al.* 2021) and studies that found the width of the biomass distribution to be narrower under warmer spring conditions across nine years in the Netherlands (Visser *et al.* 2006) and across 19 sites in the UK (Smith *et al.* 2011). However, all previous studies are low-powered ($n \leq 20$) and relied on a two-step analytical approach whereby phenological parameters were estimated for each site-year combination and then estimates were treated as data in a subsequent model, ignoring measurement error. This two-step approach will underestimate the true error in slopes. One reason for the scarcity of phenological research beyond mean timing is that the field has lacked a statistical framework for directly examining the thermal sensitivity of all three parameters that govern the phenological distribution.

Spring temperatures could affect the phenological distribution of the arboreal caterpillar guild abundance throughout spring via various intraspecific and interspecific effects. Warmer temperatures have been shown to drive earlier emergence for species that overwinter as eggs

119 or larvae (Visser *et al.* 2006; Charmantier *et al.* 2008), shifting the mean timing of the guild
120 phenology. Temperature could affect the width of the phenological distribution by changing
121 intraspecific variation in larval emergence – though no effect was found in previous work on
122 *Malacosoma disstria* (Uelmen *et al.* 2016). Temperature could also affect the period over
123 which each individual feeds prior to pupation through altering the rate of development (Stamp
124 1990; Buse *et al.* 1999), which is predicted to narrow the width and reduce the duration,
125 consistent with the findings of previous work (Visser *et al.* 2006; Smith *et al.* 2011). There are
126 multiple mechanisms that could drive a relationship between temperature and the height of the
127 phenological distribution. For instance, if low temperatures presents a constraint on
128 development, an increase in temperature may increase pre- and post-emergence survival and
129 post-emergence growth (Battisti *et al.* 2005), such that increasing temperatures could increase
130 the guild abundance and distribution height. However, colder temperatures can increase the
131 starvation tolerance of caterpillars (Abarca & Lill 2015), meaning the phenological synchrony
132 between caterpillars and their host may alter the effect of temperature on the distribution height.
133 These potential mechanisms for driving change in each phenological distribution parameter are
134 not mutually exclusive. Interspecific differences in the magnitude or direction of effect for each
135 of these mechanisms would also contribute to the thermal sensitivity of the phenological
136 distribution of the full caterpillar guild.
137
138 Here we use data on temperature and caterpillar abundance throughout spring, collected at 44
139 sites across 8 years (Fig. 2), yielding 293 site-by-year combinations, to analyse the effect of
140 temperature on the phenological distribution of 8,196 arboreal caterpillars sampled from
141 37,674 branch beatings. We develop and apply a novel statistical method, using the Gaussian
142 function, to estimate the thermal sensitivity of the three parameters that govern the phenology
143 of abundance: mean timing, height and width (i.e. standard deviation) (Fig. 1). We also

examine whether estimated thermal sensitivities over space and time are consistent with a causal effect (i.e where slopes are similar in space and time (Lovell *et al.* 2023)). Finally, using derived parameters, we explore thermal sensitivity in the duration of and area under the full phenological distribution.

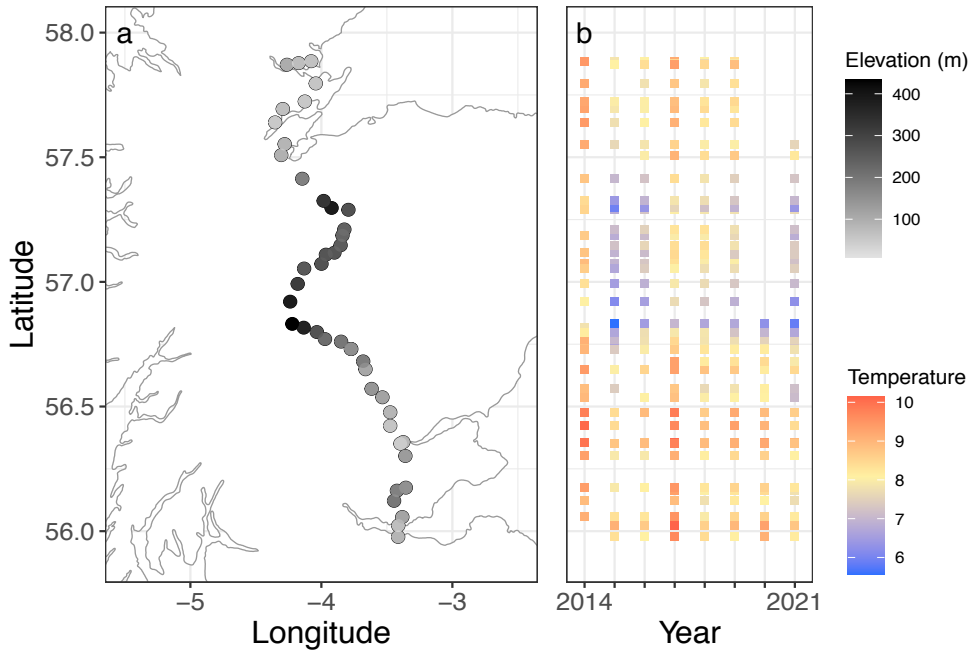

Figure 2: a) Map of site locations in Scotland with elevation above sea level indicated by a scale of grey to black, and b) shows the mean annual temperatures from mid-Feb to late June for each site in each year by latitude. Gaps in the temperature data reveal years when sites were not monitored.

Materials and Methods

Study System

Data were collected between 2014 and 2021 at 44 deciduous woodland sites along a 220km transect from Edinburgh (55°980 N, 3°400 W) to Dornoch (57°890 N, 4°080 W) in Scotland (Shutt *et al.* 2018; Macphie *et al.* 2020) (Fig. 2a). All field work was carried out with the

161 permission of site landowners. The sites vary in temperature and extend across two degrees of
162 latitude and a 440m elevation range (Fig. 2b). Two iButton temperature loggers, recording
163 hourly temperature, were installed in mid-February at different locations at each site, on the
164 north side of a tree and in a shaded area to avoid direct sunlight. The latest installation among
165 years was ordinal date 58 (27th February) and recording continued until the end of the season
166 with the earliest retrieval date among years being day 161 (9/10th June). As one site had no
167 temperature data for 2017, we used temperature data for the nearest site in 2017, making a
168 correction for the annual average difference in temperatures between the two sites.
169
170 We sampled caterpillars using a branch beating method, recording the abundance of caterpillars
171 on each branch monitored on different dates throughout spring (Shutt *et al.* 2019; Macphie *et*
172 *al.* 2020). This work defines the arboreal guild of caterpillars as the larvae of insect species
173 that spend their larval stage on deciduous trees and are similar in appearance to Lepidopterans
174 (Shutt *et al.* 2019a). Previous sampling across these sites found 93% of the guild to
175 be Lepidoptera, including 45 species: 78% of which were Geometrids (of which 45% were the
176 most common species, *Operophtera brumata*) and 13% Noctuids, and the remaining 7%
177 included species of Hymenoptera, Diptera and Coleoptera (Shutt *et al.* 2019a). At each site,
178 tree leafing phenology was monitored on a selection of trees and each year caterpillar sampling
179 began once 45% of the trees had their first leaf across all sites. The branch beating continued
180 until the end of the field season in mid/late June (2021 sampled from ordinal dates 133 to 157;
181 see Macphie *et al*. [2020] for 2014-20 details). This sampling approach captures the beginning
182 and end of the caterpillar season within the majority of site by year combinations. An average
183 of 14 trees (range: 10-17) were sampled at each site in each year from 2017-21, prior to that, 5
184 trees per site (range: 3-7) were sampled from 2014-16. One branch on each tree was marked
185 for sampling and the trees monitored represent the tree composition throughout each site,

dominated by 10 taxa: alder (*Alnus glutinosa)*, ash (*Fraxinus excelsior*), beech *(Fagus sylvatica*), birch (*Betula* spp.), elm (*Ulmus glabra*), hazel (*Corylus avellana*), oak (*Quercus* spp.), rowan (*Sorbus aucuparia*), sycamore (*Acer pseudoplatanus*) and willow (*Salix* spp.), which make up 98% of the trees sampled. Each site was visited every two days with half of the focal trees sampled on alternating visits, leaving four days between each branch beating to allow for recolonisation. The same branches were sampled across and within years unless damaged or dead.

Replication Statement

Scale of inference	**Scale at which the factor of interest is applied**	**Number of replicates at the appropriate scale**
Guild (of caterpillars)	Site by year combinations	293

Modelling the caterpillar peak as a Gaussian function

We modelled the number of caterpillars recorded on each branch as Poisson distributed with an expectation that follows a Gaussian function of scaled (mean = 147.9, sd = 14.1) ordinal date (x; Eq. 1) using the RStan package (Stan Development Team 2020). The Gaussian function (Eq. 1) is well suited to describing the phenological distribution of caterpillar abundance over time as it consists of three parameters that describe the mean timing (μ), height (A_{max}) and width (σ) (Fig. 1a) (see also Dennis *et al.* 2016 and de Villemereuil *et al.* 2020 for earlier work on phenology using the Gaussian function):

Eq. 1: $$A(x) = A_{max} exp\left(-\frac{(x-\mu)^2}{2\sigma^2}\right)$$

Eq. 1 can be rearranged into Eq. 2 allowing the height and width parameters to be modelled on the log scale:

209

210 Eq. 2: $$A(x) = exp\left(logA_{max} - \frac{(x-\mu)^2}{2exp(log\sigma)^2}\right)$$

211

212 Spatiotemporal temperature model (Fig. S1): For our main analysis we modelled $logA_{max}$,
213 $log\sigma$ and μ (the phenological parameters) using a Generalised non-linear mixed model with
214 fixed effects including an intercept and a temperature slope for each phenological parameter,
215 allowing a change in each parameter with temperature (Fig. 1b-d). The periods over which
216 mean temperatures best predicted the three phenological parameters were identified using a
217 sliding window approach (Fig. S1; see section below regarding the determination of
218 temperature predictors). The temperature variables were mean centred for the analysis and
219 differed between the phenological parameters, each comprising the mean site by year daily
220 temperatures from periods identified using the sliding window approach. Site, year and site by
221 year interaction effects were fitted as random for each phenological parameter, and the
222 covariance between the phenological parameters for each of these terms was calculated from a
223 single correlation matrix, assuming the same correlation structure among random terms, with
224 term-specific variances. Each day at each site in each year, unique tree identity, recorder of the
225 sample and each observation were also fitted as random terms for $logA_{max}$ to account for other
226 important sources of variance in caterpillar abundance (Macphie *et al.* 2020), the latter term
227 dealing with any over-dispersion with respect to the Poisson error distribution. The full analysis
228 framework is outlined in Fig. S1 in Appendix S1, Supplementary Information, and the
229 spatiotemporal model notation can be found in Appendix S2. To assess the fit of the
230 temperature slope for each phenological parameter to the parameters estimates for each site by
231 year combination we calculated a pseudo-R^2 which represents the proportion of variance
232 among site by year combinations that is explained by the slope; details can be found in
233 Appendix S3.

Where phenological data are replicated across thermal environments in space and time, it is possible to estimate separate regressions of biotic responses on temperature in both space and in time. Where the effect of temperature is similar in space and time, this increases our confidence that the effect is causal and the processes involved in space and time are similar similar (Dunne *et al.* 2004; Phillimore *et al.* 2010). Alternatively, a difference in the effect of temperature over space versus time may indicate that different processes are operating over space and time, such as local adaptation or species turnover in space but not time, or that a third variable correlated with temperature and the biotic response is at play (Tansey *et al.* 2017).

Space versus time temperature model (Fig. S1): To test for any difference in the thermal sensitivity of the caterpillar phenological distribution in space and time we included two fixed effect temperature slopes for each phenological parameter: one using the site mean temperatures and another for the annual deviations from the mean of each site (Fig. S1); employing within-site centering (Van De Pol & Wright 2009). As the among site variance in our temperature estimates is quite high, we anticipate that site estimates of mean temperatures will be quite close to the true mean and slope estimates will be largely unbiased (Phillimore *et al.* 2010; Westneat *et al.* 2020). The site mean temperatures were attained from a linear mixed-model using the lme4 package (Bates *et al.* 2015) to estimate a mean site temperature which is not biased by the years in which each site has been monitored (Fig. 2b). Separate linear mixed models were used for the temperature associated with each Gaussian function parameter and included temperature as the response variable with site and year random intercepts. The mean site temperatures from the models were mean-centred for use in the model, summarised below. The random term structure was the same as in the spatiotemporal temperature model. The difference between the spatial and temporal temperature slopes for each phenological

parameter was determined by subtracting the temporal slope estimate from the spatial slope estimate for each iteration of the posterior distributions.

Derived parameters

Duration: The width parameter is equivalent to a standard deviation, describing the curvature of the distribution, meaning that when the height is held constant a change in the width parameter defines a change in duration (Fig. 1d). When the height parameter changes with a constant width this also alters the duration (Fig. 1c), so by allowing slopes of change in both the height and the width parameters with temperature, changes in the width parameter do not uniquely define changes in duration, but this can be calculated *post-hoc*. We define the duration of the distribution as the number of days that the expected abundance exceeds some threshold. The choice of abundance threshold is arbitrary without an informed reason, and the relative difference in duration between distributions will differ depending on the threshold at which it is calculated.

Area under the phenological distribution: The formula for the area under the Gaussian function (T) can be obtained by rearranging the integral of the Gaussian function (Eq. 3) and Gaussian probability function (Eq. 4), for which the area is equal to one.

Eq. 3: $$T = \int_{-\infty}^{\infty} A_{max} exp\left(-\frac{(x-\mu)^2}{2\sigma^2}\right) dx$$

Eq. 4: $$1 = \int_{-\infty}^{\infty} \frac{1}{\sigma\sqrt{2\pi}} exp\left(-\frac{(x-\mu)^2}{2\sigma^2}\right) dx$$

$$\sigma\sqrt{2\pi} = \int_{-\infty}^{\infty} exp\left(-\frac{(x-\mu)^2}{2\sigma^2}\right) dx$$

Combining Eq. 3 and Eq.4 shows the area under the distribution can be described by Eq. 5, which rearranges to Eq. 6 when the height and width parameters are estimated on the log scale.

Eq. 5: $$T = A_{max}\sigma\sqrt{2\pi}$$

Eq. 6: $$T = exp\left(logA_{max} + log\sigma + \log\left(\sqrt{2\pi}\right)\right)$$

This shows the area under the phenological distribution depends log-linearly on temperature with a slope equal to the sum of the log-scale slope estimates for the change in height and width. Slopes for the change in the area under the distribution with changing temperature were calculated for the spatiotemporal temperature model and both components of the space vs time temperature model (Table 1).

Mean expectations on the arithmetic scale

When a variable is normally distributed on the log-scale, the mean on the arithmetic scale is equal to the sum of the log-scale mean and half of the log-scale distribution variance exponentiated. Within our models the height and width parameters are assumed to come from a log-normal distribution, meaning that the expectation on the arithmetic scale across site by years must include half of the variance attributed to the random terms being marginalised. Details of the methods of estimation on the arithmetic scale for results shown in Fig. 3 and 4 can be found in Appendix S4.

Determination of temperature predictor using sliding windows

The periods during which temperatures have most effect on the mean timing, height and width of the phenological distribution may differ among the phenological parameters; therefore, we

applied a sliding window approach simultaneously across all three parameters (Fig. S1). In the interests of efficiency we conducted model comparisons in a frequentist setting on the basis of Akaike Information Criteria (AIC) (Burnham & Anderson 2004). We obtained estimates of the mean timing, height and width of the caterpillar phenological distribution at each site in each year using the site by year model (described in Appendix S5) and then passed these estimates and a measure of measurement uncertainty to a multi-variate meta-analytic model, using the metafor package (Viechtbauer 2010). Within this framework we then ran over all combinations of sliding windows for the mean timing (start dates from 58-100 in steps of 7, durations from 28-98 days in steps of 14), height (start dates from 58-128 in steps of 14, durations from 28-98 days in steps of 14), and width (start dates from 58-128 in steps of 14, durations from 28-98 days in steps of 14), totalling 13231 models. The mean daily temperature for each site by year combination during the identified windows were then used within the Gaussian function models described above (Fig. S1).

All analyses used R version 4.0.2 (R Core Team 2020), and models including the Gaussian function used the RStan package (Stan Development Team 2020). Models were run using four chains with 2500 iterations after warmup with a thinning of 5; the spatiotemporal temperature model and space vs time model had a warmup of 2000 and the site by year model had a warmup of 1500 iterations. Convergence was checked using the Rhat (all < 1.02) and through graphical inspection. Effective sample sizes were all over 600, and over 1100 for all focal coefficients. The space vs time temperature model had 3 divergent transitions after the warmup which was 0.15% of the 2000 iterations retained. Data and code are available on Zenodo https://doi.org/10.5281/zenodo.8335050 (KHMacphie 2023).

Results

Of the 37,674 branch beatings, 3,950 of the samples recorded one or more caterpillar totalling 8,196 individuals. Of the samples in which one or more caterpillars were present, 69% recorded one and 16% recorded 2, with a maximum abundance of 109.

In the sliding window analysis, mean timing was most sensitive to temperatures from early March to mid-April (ordinal dates 65-106, 5th March - 15th April in non-leap year, Fig. 3a, S1), height was most sensitive to temperatures later in the spring (100-141, 9th April -20th May, Fig. 3a, S1) and width to temperatures that spanned the spring (58-155, 27th February - 3rd June, Fig. 3a, S1). We used the mean temperature during each of these windows as the temperature variable for the respective Gaussian parameter in in all subsequent analyses.

Spring temperatures had a significant effect on all three phenological parameters, with the most profound effects being that the caterpillar phenological distribution is both earlier and higher in warmer years (Fig. 3b-c, 4a). We found that mean timing shifted by -4.96 days $^{o}C^{-1}$ (95% credible intervals [CIs]: -6.21 - -3.64 days $^{o}C^{-1}$, Fig. 3b). The bimodal pattern among the points in Fig. 3b is caused by substantial year random effects (2014=0.25, 2016=0.62, 2017=0.25, 2018=0.11, 2019=-0.63, 2020=-0.55, 2021=-0.31 and 2022=0.24). When looking at the expected change in distribution height independently of the other parameters (see Appendix S4), the maximum abundance increased by 34% $^{o}C^{-1}$ (CIs: 5 - 61% $^{o}C^{-1}$, Fig. 3c), though we still find substantial variation in height among sites, years and site-years (Table S3; differences in phenological parameter variances among sites and years from models with and without temperature are discussed further in Appendix S6). When we account for the uncertainty in all three parameters to attain the mean expectations of abundance on each day in spring (see Appendix S4), the distribution height increased by 28% (CIs: 1 - 52%) when temperature

357 increased by one degree above the mean (Fig. 4a). The width parameter decreased by 9% $^{o}C^{-1}$

358 (CIs: 1 – 17% $^{o}C^{-1}$, Fig. 3d), indicating the shape of the distribution narrows as spring

359

360

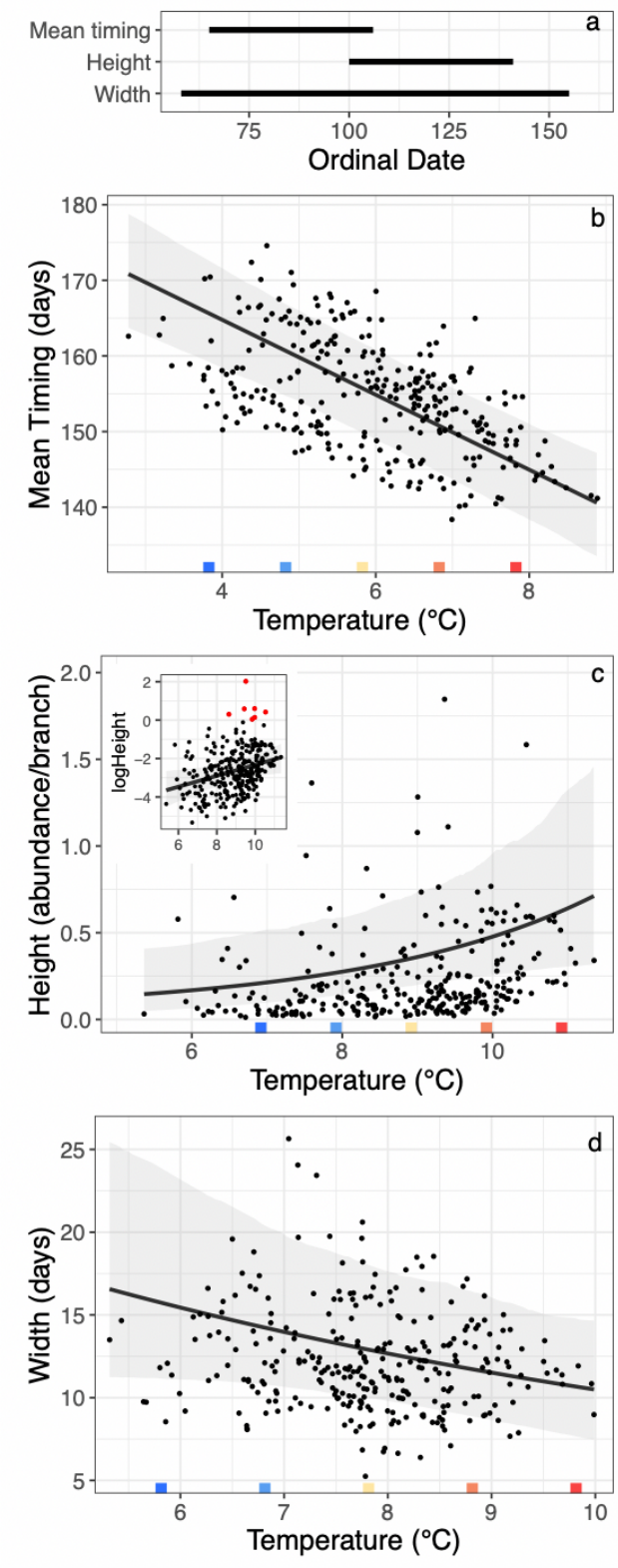

Figure 3: a) Windows of time where spring temperature was identified as the best predictor of each parameter of the phenological distribution. b-d) show the model predictions (black points) for the mean timing, height and width of the caterpillar peak, as a function of temperature during the identified windows for each site by year combination. Mean estimate on the data scale (black line) and 95% credible intervals (grey band). c) The inset plot shows log scale estimates and red points indicate points excluded from the data scale plot. Coloured squares along the x-axis show the mean temperature in yellow with +/- 1 and 2 degrees in blues/reds which correspond to the plots in Figure 4.

384 temperature increases. The temperature slopes explained 34.93% (CIs: 13.62-55.82%), 7.96%
385 (CIs: 0.15-19.17%) and 4.94% (CIs: 0.07-14.97%) of the variance among site by year
386 combinations for the mean timing, height and width parameters, respectively (Fig. 3 b-d;
387 calculations described in Appendix S3).
388
389 The duration of the distribution will be affected by both the height and width parameters and
390 varies depending on the abundance threshold at which it is calculated (Fig. 1); we therefore
391 chose to present duration at two thresholds. The purpose of quantifying duration was to assess
392 any change in the period throughout which caterpillars are present, making lower abundance
393 thresholds most informative; we chose 0.05 and 0.1 caterpillars per branch as in the absence of
394 a biological motivation the choice of abundance was arbitrary and these allowed comparison
395 across a 4ºC range (blue to red lines in Fig 4a) that is within the temperature variation we find
396 across sites and years within our study. We found no significant effect of temperature on
397 duration at either threshold across the 4ºC range within our data (Fig. 4b; mean [CIs] difference
398 between 2ºC and -2ºC at 0.1 = 19.45 days [-4.23 - 47.90]; at 0.05 = 9.42 days [-7.75 - 29.58]).
399 Whilst the change in duration at the chosen abundance levels was not significant, the mean
400 point estimates show a slight increase with temperature, particularly at the higher threshold.
401 This illustrates that whilst the shape of the peak is narrowing through a reduction in the width
402 parameter, the substantial increase in height maintains (or may even increase) the duration
403 when caterpillars are present above a particular abundance. The area under the phenological
404 distribution increases by 1.21 times per ºC (derived on the log scale then exponentiated),
405 though this effect was not significantly removed from 1 (CIs: 0.97 - 1.44, Fig. 4c).
406

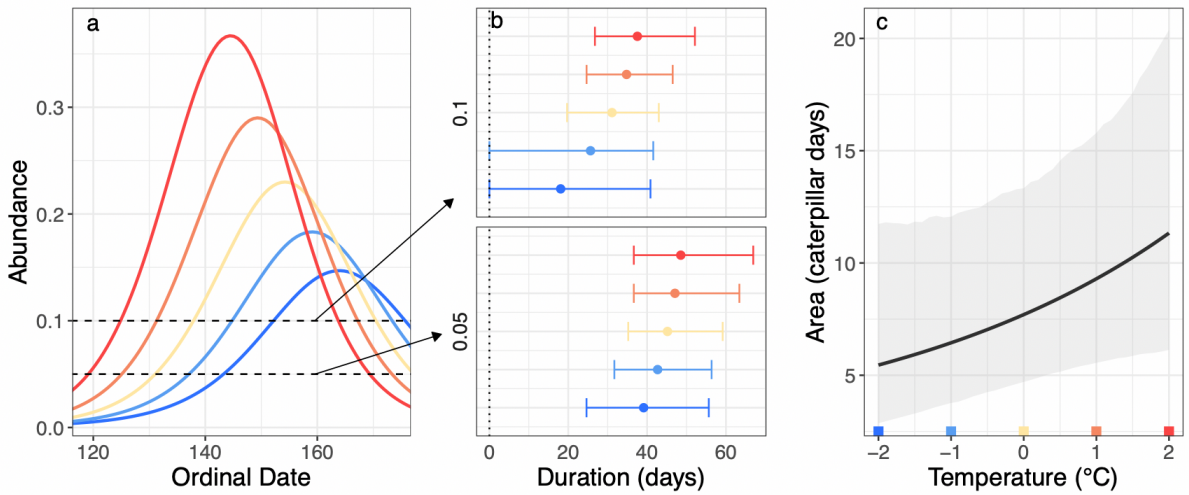

Figure 4: a) Posterior mean expected abundance on the data scale of the full phenological distribution at different temperatures: the mean of each temperature window (mean timing = 5.85°C, height = 8.92°C, width = 7.81°C; yellow), +1°C (orange), +2°C (red), -1°C (light blue) and -2°C (dark blue); calculated from the posterior predictive distribution. b) shows the mean and 95% credible intervals (95% CIs) for the duration of the peak at an abundance of 0.1 and 0.05 caterpillars for distribution at each temperature calculated from the posterior distributions of the simulated expectations of abundance across dates; and c) shows the mean and 95% CIs for the area under the phenological distribution from -2 to 2°C around the mean (centred) temperature, calculated from the simulations under the model.

Spatial and temporal slopes were generally in the same direction as the main spatiotemporal model (Table 1), except for the temporal width parameter slope. For the mean timing parameter, estimates in space and time were not significantly different and both were in the same direction with CIs removed from zero. Whilst there was no significant difference in the mean timing slopes across space and time, the difference in the point estimates were consistent with a co-gradient, a steeper spatial slope. For the thermal sensitivity of the distribution height, the spatial and temporal estimates did not significantly differ, and point estimates were in the same direction consistent with a co-gradient pattern; however the credible intervals for both terms included 0. The thermal sensitivity of the width parameter was significantly different in

space versus time, with a significant negative spatial slope, but no effect of temperature across years. The effect of temperature on the area under the phenological distribution was similar in the main model and over space and time, all showing positive but non-significant effects.

Table 1: Summary of results for the effect of temperature on the mean timing, height, width and area under the phenological distribution of spring arboreal caterpillars, showing posterior mean effect with 95% credible intervals (CI) in brackets beneath. Spatiotemporal slopes come from a model using temperatures for each site-year to estimate the thermal sensitivity of the parameters. The spatial and temporal slopes come from a model employing a within-site centering approach to separate the effects in space and time. The difference column indicates the difference between the spatial and temporal slope estimates calculated from the spatial slope minus the temporal. Slope estimates are exponentiated or unscaled where applicable and 'prop.' in the unit column implies proportional changes (i.e. exponentiated slopes). For the mean timing parameter and the difference column CI removal from 0 suggests a significant effect, whereas for the three parameters in units of proportional change CI removal from 1 suggests significance.

Parameter	Unit	Spatiotemporal slope	Spatial slope	Temporal slope	Difference (S-T)
Mean Timing	days $^{o}C^{-1}$	-4.96 (-6.21 - -3.64)	-5.77 (-7.39 - -4.18)	-3.39 (-5.49 - -1.46)	-2.37 (-4.77 - 0.17)
Height	prop. change $^{o}C^{-1}$	1.34 (1.05 - 1.61)	1.66 (0.97 - 2.63)	1.17 (0.81 - 1.49)	0.49 (-0.31 - 1.55)
Width	prop. change $^{o}C^{-1}$	0.91 (0.83 - 0.99)	0.85 (0.75 - 0.96)	1.05 (0.89 - 1.21)	-0.20 (-0.39 - -0.01)
Area	prop. change $^{o}C^{-1}$	1.21 (0.97 - 1.44)	1.40 (0.90 - 2.12)	1.22 (0.89 - 1.53)	0.18 (-0.41 - 0.95)

Discussion

We found that spring temperatures have an effect on the mean timing, height and width of the caterpillar phenological distribution. In addition to the phenological mean timing shifting by -4.96 days $^{o}C^{-1}$, which is consistent with results from previous studies (Visser *et al.* 2006; Charmantier *et al.* 2008; Burgess *et al.* 2018), the distribution height increases by 34% $^{o}C^{-1}$ and decreases in width by 9% $^{o}C^{-1}$ (Fig 3b-d). Whilst the shape of the peak narrows through the decrease in width, when paired with the substantial increase in height we found no change in the duration of the distribution with changing temperature (Fig 4b). The results reveal substantial thermal sensitivity of the full phenological distribution, including effects that have been largely overlooked in earlier work on phenology and MMH research.

Our finding that spring temperatures have a substantial impact on the maximum height of the caterpillar guild phenological distribution (an increase of 34% $^{o}C^{-1}$) is likely to have cascading effects through interactions within the forest community. Even an increase in temperature of 1.5^{o}C could yield more than a 50% increase in the maximum abundance of arboreal caterpillars. This is liable to lead to an increase in herbivory pressure that represents a potentially major indirect effect of temperature on the severity of tree defoliation (Kulman 1971; Whittaker & Warrington 1985; Whitham *et al.* 1991; Marquis & Whelan 1994), though this effect will also depend on the thermal sensitivity of leaf toughness and palatability. The impact on tree defoliation and growth is likely to depend on how synchronous caterpillars are to the tree and the level of defences the leaves have acquired at the time of maximum herbivory (Schwartzberg *et al.* 2014; Bellemin-Noël *et al.* 2021). Should the increased maximum abundance translate to a greater prevalence of pest outbreaks and defoliation, further work into whether the change is driven by a few specific species or is consistent throughout the guild will be important for the

468 design of effective and targeted pest management interventions. An increase in the height of
469 the caterpillar phenological distribution is also liable to have profound consequences for
470 secondary consumers, a theme to which we will return.
471
472 The positive effect of spring temperature on the height of phenological abundance distribution
473 that we observe departs substantially from the Nadolski et al. (2021) report of no correlation
474 between annual temperature variation and maximum caterpillar biomass in Poland across 16
475 years. Whilst it is possible that this reflects true differences in the caterpillar thermal-response
476 between Scotland and Poland, perhaps influenced by spatial patterns in the thermal sensitivity
477 of defoliator populations (Netherer & Schopf 2010), it is possible that our slopes do not in fact
478 differ from theirs. Whilst Nadolski et al. do not report a slope or confidence interval, the
479 interval is likely to be broad and therefore may overlap with our result.
480
481 By separating the effects of temperature in space and time we can gain a window into whether
482 effects are likely to be causal and insights into the processes at play (Lovell *et al.* 2023). For
483 the mean timing parameter, similar estimates in space and time suggest temperature has a
484 causal effect and is consistent with plasticity being responsible for much of the spatiotemporal
485 variation in mean timing (Phillimore *et al.* 2010). While non-significant, the difference in the
486 point estimates was in a direction consistent with a co-gradient pattern, which may suggest
487 some contribution of local adaptation or a difference in species turnover over space versus over
488 time. For the thermal sensitivity of the distribution height, the general direction of the estimates
489 and lack of difference in space versus time suggests a causal effect of temperature, with a
490 possible co-gradient pattern; yet neither effect was significant when considered in isolation.
491 For the thermal sensitivity of the width, the lack of a trend in time but significant negative
492 effect in space were consistent with the findings of Smith et al (2011). Such a difference

493 between effects estimated over space and time suggests a non-causal relationship between
494 temperature and distribution width in our main model. The positive but non-significant effect
495 of temperature on the area under the phenological distribution was similar in both space and
496 time and the spatiotemporal model; we therefore cannot conclude that there is any effect of
497 temperature on the area under the curve within our data set, though this presents an interesting
498 avenue for future work. While point estimates for all temperature-phenology effects are in the
499 same direction over space and time, the trends are estimated with considerable uncertainty and
500 we suggest there would be value in revisiting these analyses with greater temporal replication
501 in the future.
502
503 Our spatiotemporal estimate of a shift in phenological mean of -4.96 days$^{o}C^{-1}$ in the caterpillar
504 guild is similar to estimates obtained for leaf out in oak trees and other deciduous species from
505 previous studies across Europe (Vitasse *et al.* 2010; Roberts *et al.* 2015; Tansey *et al.* 2017).
506 In contrast, our estimate of the temporal slope for mean caterpillar timing is shallower than
507 some dominant UK trees, e.g., *Quercus* sp. leaf-out found to have sensitivity to forcing
508 temperatures of -8.81 +/- 0.52 days $^{o}C^{-1}$ (Roberts *et al.* 2015). This means that increasing
509 temperatures could alter the phenological (a)synchrony between caterpillars and deciduous
510 trees, despite previous studies suggesting that caterpillars are maintaining synchrony with oak
511 (Both *et al.* 2009; Burgess *et al.* 2018). An increase in tree-caterpillar asynchrony may impede
512 the increase in the height of the caterpillar phenological distribution and prevent the most
513 extreme detrimental effects for the trees (Schwartzberg *et al.* 2014), whilst greater synchrony
514 could exacerbate the increase in herbivory pressure (Schwartzberg *et al.* 2014; Bellemin-Noël
515 *et al.* 2021).
516

517 Moving up the food chain to the insectivorous bird-caterpillar trophic interaction, a study of
518 bird species in UK and Netherlands (not limited to woodland passerines) showed an average
519 advance in lay date of 3.28 days $^{o}C^{-1}$ for resident species and 2.49 days $^{o}C^{-1}$ for migratory
520 species (Mclean *et al.* 2022). Our temporal estimate for the shift in caterpillar mean timing is
521 similar to the estimate for resident birds and the average migratory species slope falls within
522 the temporal caterpillar slope CIs (Mclean *et al.* 2022). The overlap between bird and
523 caterpillar slope estimates suggests that average resident and migratory bird species may be
524 able to track the change in caterpillar phenology from year to year.
525
526 Where the thermal sensitivity of phenology differs between trophic levels (Thackeray *et al.*
527 2016), changing temperatures will alter the asynchrony between a consumer and its resource
528 (Kharouba *et al.* 2018). The MMH is most often studied through comparison of consumer
529 phenology and fitness to the resource population/guild mean timing; yet the height and width
530 of the resource distribution determines the duration of time for which the resource is above a
531 given threshold, the amount of food available i) as the total among days throughout spring (the
532 area under the phenological distribution) or ii) given a particular amount of phenological
533 asynchrony and how the relative amount of food available differs among synchronous and
534 asynchronous consumers. For forest birds that rely on caterpillars as a food resource to feed
535 nestlings, the impacts of temperature on the shape and height of the caterpillar peak could have
536 stark consequences for how the MMH manifests. The increase in peak height means that under
537 warmer spring conditions far more food is predicted to be available to consumers that remain
538 approximately synchronous with the caterpillars. However, the reduction in peak width with
539 increasing temperature means that resource abundance declines more steeply to either side of
540 the mean timing under warmer conditions, affecting the relative abundance of food available
541 to synchronous versus asynchronous consumers. Therefore, the fitness consequences of

asynchrony could change with temperature, potentially increasing the strength of stabilising or directional selection on consumer breeding phenology. In the future, the modelling framework we present here could be extended to model the impact of the three phenological parameters of the resource on the parameters that govern the phenological fitness function of consumers (or resources). Specifically under the MMH we predict that the mean timing, height and width of the resource should have causal effects on the optimum timing, maximum and width of the consumer phenological fitness function (Macphie 2023).

Through allowing temperature during different windows to affect each distribution parameter in the sliding window we have gained new insights into the thermal sensitivity of the caterpillar phenological distribution. The window identified as most influential for mean timing falls prior to the onset of the main peak in abundance, most likely influencing hatching phenology rather than altering the mean timing through impact on developmental rate, and is similar to that identified as important in other European studies (Visser *et al.* 2006; Porlier *et al.* 2012; Simmonds *et al.* 2020). The height of the distribution however is most sensitive to temperatures around the onset of the peak and in the weeks following, suggesting the thermal sensitivity in height is driven more by thermal effects on the larvae (and potentially their host plants) than eggs. For width our time window is broader than identified in Visser et al (2006), though we note a high degree of uncertainty in the position of the window for this phenological parameter (Fig. S2). The sliding window approach involves a very high-level of multiple testing (13231 window combinations in our case) (van de Pol *et al.* 2016), which inflates the type I errors. In the context of our study, we anticipate that this is most likely to affect the slope of temperature on the width parameter, which is the weakest of the correlations we identify. It is also possible that the most influential window of temperature will differ with elevation and latitude (Macphie 2023), or that the window that affects height and width may be relative to caterpillar phenology.

Our approach is similar to the Gaussian model functions described in de Villemereuil et al. (2020) and Dennis et al. (2016), with the major difference being that we include linear effects of temperature on the three parameters that control the position, shape and height of the phenological distribution. The approach we present here offers great potential for modelling effects of climate (e.g., temperature, precipitation) or other continuous variables (e.g., year, density of conspecifics) on phenological distributions. Examples of seasonal events that could be approximated by a Gaussian phenological distribution include planktonic blooms, tree leafing and senescence, flowering, fruiting, fish or amphibian spawning events, migration and reproduction metrics for mammals or birds, and numbers of parasitised or diseased individuals. Further potential improvements to the approach include modelling of skewed phenological distributions and incorporation of spatiotemporal autocorrelation in parameters (particularly height, as abundance is expected to be correlated from one year to the next). In addition, inclusion of linear latitude and year effects would reduce the risk that the effects that we attribute to climate variables arise from third variables that exhibit spatial or temporal trends. The approach we describe has advantages over use of a GLM/GLMM with a Poisson response and quadratic date term to estimate the effects of an environmental variable on mean timing (Chevin *et al.* 2015; Edwards & Crone 2021), as we found that this approach forces an undesirable non-linear relationship between the environmental variable and height (see Appendix S7 for further details).

Introducing a new approach for estimating climate-phenology relationships, we have shown that temperature has an effect not only on the mean timing of the phenological distribution of spring arboreal caterpillars, but also on the height and width of the peak. We report an increase in the height accompanied by a decrease in the width; resulting in a similar duration of the

592 distribution as temperature increases. The alterations to the shape of the phenological
593 distribution of caterpillars not only identifies shifts in dynamics within the caterpillar guild that
594 are attributed to temperature, but it will also impact the herbivory pressure on deciduous trees
595 and alter the food availability throughout spring for breeding birds with possible implications
596 for the MMH. The methods we present have broad applicability to other systems and questions
597 within phenology and the MMH, and we encourage more work to consider the full
598 phenological distribution of biological events rather than focusing on mean timing. To predict
599 the biotic impacts of ongoing climate warming, it will often be essential to take these additional
600 components of change into account.

601

602

603 **Author Contributions:**

604 KHM, ABP and JMS collected the data. KHM, ABP and JDH designed the analyses. KHM
605 conducted the analyses with input from JDH and JLP. KHM wrote the first draft and all authors
606 contributed to editing and revisions.

607

608 **Acknowledgements:**

609 We are very grateful to Jack Shutt and many field assistants for data collection, to Wolfgang
610 Viechtbauer for support in using the metafor package, Rebecca Lovell and Jamie Weir for
611 comments and to the landowners of the sites on which we work. This work was funded by a
612 Natural Environment Research Council (NERC) advanced fellowship (NE/I020598/1O) and
613 NERC grant no. (NE/P011802/1) and a NERC E3 DTP PhD to K.H.M. For the purpose of
614 open access, the author has applied a Creative Commons Attribution (CC BY) licence to any
615 Author Accepted Manuscript version arising from this submission.

616

References

Abarca, M. & Lill, J.T. (2015). Warming affects hatching time and early season survival of eastern tent caterpillars. *Oecologia*, 179, 901–912.

Ahmad, M., Uniyal, S.K., Batish, D.R., Rathee, S., Sharma, P. & Singh, H.P. (2021). Flower phenological events and duration pattern is influenced by temperature and elevation in Dhauladhar mountain range of Lesser Himalaya. *Ecol. Indic.*, 129, 107902.

Bates, D., Mächler, M., Bolker, B. & Walker, S. (2015). Fitting Linear Mixed-Effects Models Using lme4. *J. Stat. Softw.*, 67, 1–48.

Battisti, A., Stastny, M., Netherer, S., Robinet, C., Schopf, A., Roques, A., *et al.* (2005). Expansion of geographic range in the pine processionary moth caused by increased winter temperatures. *Ecol. Appl.*, 15, 2084–2096.

Bellemin-Noël, B., Bourassa, S., Despland, E., De Grandpré, L. & Pureswaran, D.S. (2021). Improved performance of the eastern spruce budworm on black spruce as warming temperatures disrupt phenological defences. *Glob. Chang. Biol.*, 27, 3358–3366.

Bock, A., Sparks, T.H., Estrella, N., Jee, N., Casebow, A., Schunk, C., *et al.* (2014). Changes in first flowering dates and flowering duration of 232 plant species on the island of Guernsey. *Glob. Chang. Biol.*, 20, 3508–3519.

Both, C., van Asch, M., Bijlsma, R.G., van den Burg, A.B. & Visser, M.E. (2009). Climate change and unequal phenological changes across four trophic levels: constraints or adaptations? *J. Anim. Ecol.*, 78, 73–83.

Bowler, D.E., Hof, C., Haase, P., Kröncke, I., Schweiger, O., Adrian, R., *et al.* (2017). Cross-realm assessment of climate change impacts on species' abundance trends. *Nat. Ecol. Evol. 2017 13*, 1, 1–7.

Buckley, L.B., Graham, S.I. & Nufio, C.R. (2021). Grasshopper species' seasonal timing underlies shifts in phenological overlap in response to climate gradients, variability and

change. *J. Anim. Ecol.*, 90, 1252–1263.

Burgess, M.D., Smith, K.W., Evans, K.L., Leech, D., Pearce-Higgins, J.W., Branston, C.J., *et al.* (2018). Tritrophic phenological match–mismatch in space and time. *Nat. Ecol. Evol.*, 2, 970–975.

Burnham, K.P. & Anderson, D.R. (2004). Multimodel inference: understanding AIC and BIC in model selection. *Sociol. Methods Res.*, 33, 261–304.

Buse, A., Dury, S.J., Woodburn, R.J.W., Perrins, C.M. & Good, J.E.G. (1999). Effects of elevated temperature on multi-species interactions: the case of Pedunculate Oak, Winter Moth and Tits. *Funct. Ecol.*, 13, 74–82.

Charmantier, A., McCleery, R.H., Cole, L.R., Perrins, C., Kruuk, L.E.B. & Sheldon, B.C. (2008). Adaptive phenotypic plasticity in response to climate change in a wild bird population. *Science (80-.).*, 320, 800–3.

Chevin, L.-M., Visser, M.E. & Tufto, J. (2015). Estimating the variation, autocorrelation, and environmental sensitivity of phenotypic selection. *Evolution (N. Y).*, 69, 2319–2332.

Cohen, J.M., Lajeunesse, M.J. & Rohr, J.R. (2018). A global synthesis of animal phenological responses to climate change. *Nat. Clim. Chang.*, 8, 224–228.

Cole, E.F., Regan, C.E. & Sheldon, B.C. (2021). Spatial variation in avian phenological response to climate change linked to tree health. *Nat. Clim. Chang.*, 11, 872–878.

Cushing, D.H. (1969). The Regularity of the Spawning Season of Some Fishes. *ICES J. Mar. Sci.*, 33, 81–92.

Dennis, E.B., Morgan, B.J.T., Freeman, S.N., Roy, D.B. & Brereton, T. (2016). Dynamic Models for Longitudinal Butterfly Data. *J. Agric. Biol. Environ. Stat.*, 21, 1–21.

Dunne, J.A., Saleska, S.R., Fischer, M.L. & Harte, J. (2004). Integrating experimental and gradient methods in ecological climate change research. *Ecology*, 85, 904–916.

Edwards, C.B. & Crone, E.E. (2021). Estimating abundance and phenology from transect

667 count data with GLMs. *Oikos*, 130, 1335–1345.
668 Hällfors, M.H., Antão, L.H., Itter, M., Lehikoinen, A., Lindholm, T., Roslin, T., *et al.* (2020).
669 Shifts in timing and duration of breeding for 73 boreal bird species over four decades.
670 *Proc. Natl. Acad. Sci.*, 117, 18557–18565.
671 Kharouba, H.M., Ehrlén, J., Gelman, A., Bolmgren, K., Allen, J.M., Travers, S.E., *et al.*
672 (2018). Global shifts in the phenological synchrony of species interactions over recent
673 decades. *Proc. Natl. Acad. Sci.*, 115, 5211–5216.
674 KHMacphie. (2023). KHMacphie/CaterPeakTemp: Modelling thermal sensitivity in the full
675 phenological distribution (v1.0). *Zenodo*, https://doi.org/10.5281/zenodo.8335050.
676 Kulman, H.M. (1971). Effects of insect defoliation on growth and mortality of trees. *Annu.*
677 *Rev. Entomol.*, 16, 289–324.
678 Lovell, R.S., Collins, S., Martin, S.H., Pigot, A.L. & Phillimore, A.B. (2023). Space-for-time
679 substitutions in climate change ecology and evolution. *Biol. Rev.*
680 Macphie, K.H. (2023). The full phenological distribution and the match/mismatch
681 hypothesis.
682 Macphie, K.H., Samplonius, J.M., Hadfield, J., Higgins, J.W.P. & Phillimore, A. (2020).
683 Among tree and habitat differences in the timing and abundance of spring caterpillars.
684 *EcoEvoRxiv*, 1–53.
685 Marquis, R.J. & Whelan, C.J. (1994). Insectivorous Birds Increase Growth of White Oak
686 through Consumption of Leaf-Chewing Insects. *Ecology*, 75, 2007–2014.
687 Mclean, N., Kruuk, L.E.B., Van Der Jeugd, H.P., Leech, D., Van Turnhout, C.A.M. & Van
688 De Pol, M. (2022). Warming temperatures drive at least half of the magnitude of long-
689 term trait changes in European birds. *Proc. Natl. Acad. Sci.*, 16.
690 Møller, A.P., Flensted-Jensen, E., Klarborg, K., Mardal, W. & Nielsen, J.T. (2010). Climate
691 change affects the duration of the reproductive season in birds. *J. Anim. Ecol.*, 79, 777–

784.

Nadolski, J., Marciniak, B., Loga, B., Michalski, M. & Bańbura, J. (2021). Long-term variation in the timing and height of annual peak abundance of caterpillars in tree canopies: Some effects on a breeding songbird. *Ecol. Indic.*, 121, 107120.

Netherer, S. & Schopf, A. (2010). Potential effects of climate change on insect herbivores in European forests—General aspects and the pine processionary moth as specific example. *For. Ecol. Manage.*, 259, 831–838.

Parmesan, C. & Yohe, G. (2003). A globally coherent fingerprint of climate change impacts across natural systems. *Nature*, 421, 37–42.

Phillimore, A.B., Hadfield, J.D., Jones, O.R. & Smithers, R.J. (2010). Differences in spawning date between populations of common frog reveal local adaptation. *PNAS*, 107, 8292–8297.

van de Pol, M., Bailey, L.D., McLean, N., Rijsdijk, L., Lawson, C.R. & Brouwer, L. (2016). Identifying the best climatic predictors in ecology and evolution. *Methods Ecol. Evol.*, 7, 1246–1257.

Van De Pol, M. & Wright, J. (2009). A simple method for distinguishing within- versus between-subject effects using mixed models. *Anim. Behav.*, 753–758.

Porlier, M., Charmantier, A., Bourgault, P., Perret, P., Blondel, J. & Garant, D. (2012). Variation in phenotypic plasticity and selection patterns in blue tit breeding time: between- and within-population comparisons. *J. Anim. Ecol.*, 81, 1041–1051.

R Core Team. (2020). R: A language and environment for statistical computing. R Foundation for Statistical Computing, Vienna, Austria. URL https://www.R-project.org/.

Reed, T.E., Jenouvrier, S. & Visser, M.E. (2013). Phenological mismatch strongly affects individual fitness but not population demography in a woodland passerine. *J. Anim. Ecol.*, 82, 131–144.

717 Roberts, A.M.I., Tansey, C., Smithers, R.J. & Phillimore, A.B. (2015). Predicting a change in
718 the order of spring phenology in temperate forests. *Glob. Chang. Biol.*, 21, 2603–2611.
719 Roslin, T., Antão, L., Hällfors, M., Meyke, E., Lo, C., Tikhonov, G., *et al.* (2021).
720 Phenological shifts of abiotic events, producers and consumers across a continent. *Nat.*
721 *Clim. Chang.*, 11, 241–248.
722 Samplonius, J.M., Atkinson, A., Hassall, C., Keogan, K., Thackeray, S.J., Assmann, J.J., *et*
723 *al.* (2020). Strengthening the evidence base for temperature-mediated phenological
724 asynchrony and its impacts. *Nat. Ecol. Evol.*, 5, 155–164.
725 Schwartzberg, E.G., Jamieson, M.A., Raffa, K.F., Reich, P.B., Montgomery, R.A. &
726 Lindroth, R.L. (2014). Simulated climate warming alters phenological synchrony
727 between an outbreak insect herbivore and host trees. *Oecologia*, 175, 1041–1049.
728 Shutt, J.D., Bolton, M., Cabello, I.B., Burgess, M.D. & Phillimore, A.B. (2018). The effects
729 of woodland habitat and biogeography on blue tit (Cyanistes caeruleus) territory
730 occupancy and productivity along a 220km transect. *Ecography (Cop.).*, 1–12.
731 Shutt, J.D., Burgess, M.D. & Phillimore, A.B. (2019). A spatial perspective on the
732 phenological distribution of the spring woodland caterpillar peak. *Am. Nat.*, 194, E109–
733 E121.
734 Simmonds, E.G., Cole, E.F., Sheldon, B.C. & Coulson, T. (2020). Phenological asynchrony:
735 a ticking time-bomb for seemingly stable populations? *Ecol. Lett.*, 23, 1766–1775.
736 Smith, K.W., Smith, L., Charman, E., Briggs, K., Burgess, M., Dennis, C., *et al.* (2011).
737 Large-scale variation in the temporal patterns of the frass fall of defoliating caterpillars
738 in oak woodlands in Britain: implications for nesting woodland birds. *Bird Study* , 58,
739 506–511.
740 Stamp, N.E. (1990). Growth versus molting time of caterpillars as a function of temperature,
741 nutrient concentration and the phenolic rutin. *Oecologia*, 82, 107–113.

742 Stan Development Team. (2020). RStan: the R interface to Stan. R package version 2.21.2.
743 http://mc-stan.org/.
744 Tansey, C.J., Hadfield, J.D. & Phillimore, A.B. (2017). Estimating the ability of plants to
745 plastically track temperature-mediated shifts in the spring phenological optimum. *Glob.*
746 *Chang. Biol.*, 23, 3321–3334.
747 Thackeray, S.J., Henrys, P.A., Hemming, D., Bell, J.R., Botham, M.S., Burthe, S., *et al.*
748 (2016). Phenological sensitivity to climate across taxa and trophic levels. *Nature*, 535,
749 241–245.
750 Thomas, D.W., Blondel, J., Perret, P., Lambrechts, M.M. & Speakman, J.R. (2001).
751 Energetic and Fitness Costs of Mismatching Resource Supply and Demand in
752 Seasonally Breeding Birds. *Science (80-.).*, 291, 2598–2600.
753 Uelmen, J.A., Lindroth, R.L., Tobin, P.C., Reich, P.B., Schwartzberg, E.G. & Raffa, K.F.
754 (2016). Effects of winter temperatures, spring degree-day accumulation, and insect
755 population source on phenological synchrony between forest tent caterpillar and host
756 trees. *For. Ecol. Manage.*, 362, 241–250.
757 Viechtbauer, W. (2010). Conducting meta-analyses in R with the metafor package. *J. Stat.*
758 *Softw.*, 36, 1–48.
759 de Villemereuil, P., Charmantier, A., Arlt, D., Bize, P., Brekke, P., Brouwer, L., *et al.* (2020).
760 Fluctuating optimum and temporally variable selection on breeding date in birds and
761 mammals. *Proc. Natl. Acad. Sci.*, 117, 31969–31978.
762 Visser, M.E., Holleman, L.J.M. & Gienapp, P. (2006). Shifts in caterpillar biomass
763 phenology due to climate change and its impact on the breeding biology of an
764 insectivorous bird. *Oecologia*, 147, 164–172.
765 Vitasse, Y., Bresson, C.C., Kremer, A., Michalet, R. & Delzon, S. (2010). Quantifying
766 phenological plasticity to temperature in two temperate tree species. *Funct. Ecol.*, 24,

1211–1218.

Vitasse, Y., Porté, A.J., Kremer, A., Michalet, R. & Delzon, S. (2009). Responses of canopy duration to temperature changes in four temperate tree species: relative contributions of spring and autumn leaf phenology. *Oecologia*, 161, 187–198.

Walther, G.-R., Post, E., Convey, P., Menzel, A., Parmesan, C., Beebee, T.J.C., *et al.* (2002). Ecological responses to recent climate change. *Nature*, 416, 389–395.

Westneat, D.F., Araya-Ajoy, Y.G., Allegue, H., Class, B., Dingemanse, N., Dochtermann, N.A., *et al.* (2020). Collision between biological process and statistical analysis revealed by mean centring. *J. Anim. Ecol.*, 89, 2813–2824.

Whitham, T.G., Maschinski, J., Larson, K.D. & Paige, K.N. (1991). Plant responses to herbivory : the continuum from negative to positive and underlying physiological mechanisms. In: *Plant-Animal Interactions : Evolutionary Ecology in Tropical and Temperate Regions*. John Wiley & Sons, New York, New York, USA., pp. 227–256.

Whittaker, J.B. & Warrington, S. (1985). An Experimental Field Study of Different Levels of Insect Herbivory Induced By Formica rufa Predation on Sycamore (Acer pseudoplatanus) III. Effects on Tree Growth. *J. Appl. Ecol.*, 22, 797–811.

Modelling thermal sensitivity in the full phenological distribution: a new approach applied to the spring arboreal caterpillar peak

Functional Ecology

Kirsty H. Macphie[1*], Jelmer M. Samplonius[1], Joel L. Pick[1], Jarrod D. Hadfield[1], Albert B. Phillimore[1]

[1] Institute for Ecology and Evolution, The University of Edinburgh, Edinburgh, UK

Supplementary Information

Contents

808 **Appendix S1: Framework summary figure**

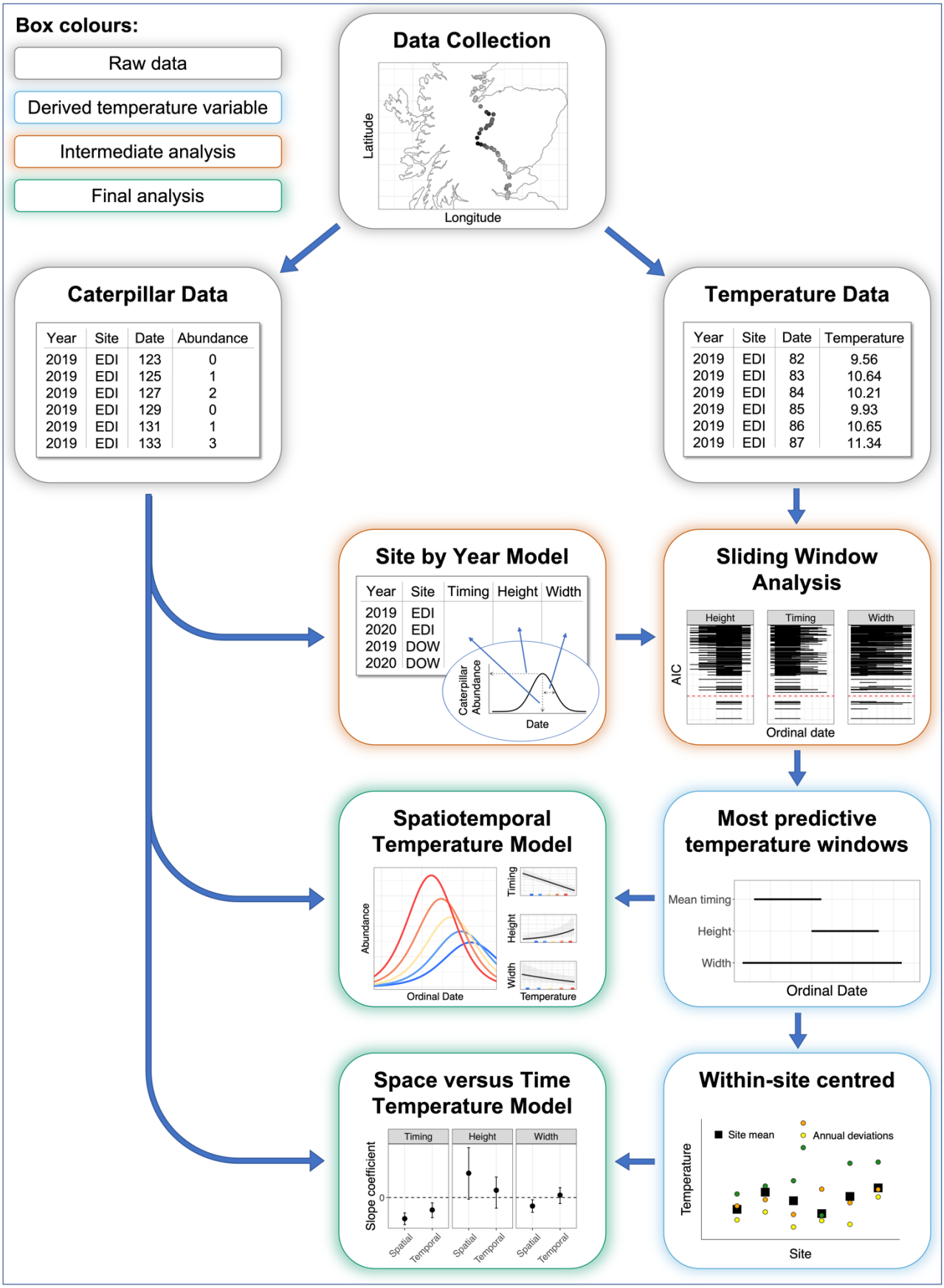

Figure S1: Graphical outline of the methodological framework used to analyse the effect of temperature on the full phenological distribution. Raw data on the abundance of caterpillars on days throughout spring (**Caterpillar Data**) and daily mean temperatures (**Temperature Data**) were collected at each site over multiple years. The caterpillar data were used to estimate the mean timing, height and width of the phenological distribution at each site in each year (**Site by Year Model**). A multi-variate meta-analytical **Sliding Window Analysis** was used to estimate the **most predictive temperature windows**, allowing a separate window for each phenological distribution parameter. The **Spatiotemporal Temperature Model** used site-by-year variation in average temperatures from these windows as predictors of each phenological distribution parameter estimated using raw caterpillar data (modelled as a Gaussian function of ordinal date). Site-by-year temperatures were **within-site centred**, with the site mean temperature and annual temperature deviations used as predictors of each phenological parameter in the **Space versus Time Model** (following the same approach as the spatiotemporal model).

Appendix S2: Spatiotemporal temperature model notation

The abundance of caterpillars, y, recorded at the ith site in the jth year on the kth date and tth tree by the rth recorder was Poisson distributed with mean λ:

Eq. S1: $y_{ijktr} \sim Pois(\lambda_{ijktr})$

λ was modelled as a Gaussian function of ordinal date x in which the phenological parameters, m, A_{max}, and σ define the mean timing, height and width respectively. On the log-scale this model is:

Eq. S2: $$log(\lambda_{ijktr}) = logA_{max} - \frac{(x-m)^2}{2\sigma^2} + e_{ijktr}$$

where e_{ijktr} is an observation-level random effect that captures any overdispersion with respect to the Poisson. Each phenological parameter (or in the case of A_{max}, and σ, their log) follows a linear model with an intercept β_1 and a slope with respect to temperature β_2 as fixed effects. Note different temperature variables are used for each phenological parameter since different time windows over which temperature was averaged were selected. In addition, site $u^{(s)}$ year $u^{(y)}$ and site by year $u^{(s:y)}$ random terms were included. The linear model for $logA_{max}$ also included random terms for date by site by year $u^{(x:s:y)}$, tree identity $u^{(t)}$ and sample recorder $u^{(r)}$.

Eq. S3: $$m = \beta_1^{(m)} + \beta_2^{(m)} t_{ij}^{(m)} + u_i^{(m:s)} + u_j^{(m:y)} + u_{ij}^{(m:s:y)}$$

Eq. S4: $$logA_{max} = \beta_1^{(h)} + \beta_2^{(h)} t_{ij}^{(h)} + u_i^{(h:s)} + u_j^{(h:y)} + u_{ij}^{(h:s:y)} + u_{ijk}^{(h:x:s:y)} + u_t^{(h:t)} + u_r^{(h:r)}$$

Eq. S5: $$log\sigma = \beta_1^{(w)} + \beta_2^{(w)} t_{ij}^{(w)} + u_i^{(w:s)} + u_j^{(w:y)} + u_{ij}^{(w:s:y)}$$

The vector containing the three (one for each phenological parameter) site effects for site i $\mathbf{u}_i^{(s)}$ were drawn from a normal distribution with a zero mean vector and a variance-covariance matrix estimated from $\mathbf{D}^{(s)}\mathbf{R}\mathbf{D}^{(s)}$ in which $\mathbf{D}^{(s)}$ represents a diagonal matrix with the standard deviations of the site random effects along the diagonal and **R** represents the correlation matrix for the three terms:

Eq. S6: $$\begin{bmatrix} u_i^{(m:s)} \\ u_i^{(h:s)} \\ u_i^{(w:s)} \end{bmatrix} \sim N\left(\begin{bmatrix} 0 \\ 0 \\ 0 \end{bmatrix}, \mathbf{D}^{(s)}\mathbf{R}\mathbf{D}^{(s)}\right)$$

The vectors of year and site by year effects, $\mathbf{u}_j^{(y)}$ and $\mathbf{u}_{ij}^{(y)}$ respectively, were modelled in the same way, with **R** common to the site, year, and site by year effects but with effect-specific standard deviations (i.e. $\mathbf{D}^{(y)}$ and $\mathbf{D}^{(s:y)}$).

Appendix S3: Pseudo-R^2 for phenological parameter-temperature slopes

To give some indication of the model fit for the main slope effect results shown in Fig. 3b-d, we calculated the proportion of variance among site by year combinations that is explained by the slope:

Eq. S7: $$R^{2(m)} = \frac{\beta_2^{2(m)} var(t^{(m)})}{\beta_2^{2(m)} var(t^{(m)}) + var(u^{(m:s)}) + var(u^{(m:y)}) + var(u^{(m:s:y)})}$$

The slope coefficient squared β_2^2 multiplied by the variance in site by year temperature $var(t_{ij})$ gives the variance explained by the slope. The variance explained by the slope is divided by the total variance among site by year combinations, which consists of the variance explained by the slope and the remaining variance attributed to site, year and site by year random terms. Eq. S7 shows the equation for the mean timing parameter m, the same is used for the height and width parameter "R^2" estimates.

Appendix S4: Mean expectation on the arithmetic scale

There are two forms of expectations on the arithmetic scale that we were interested in from the spatiotemporal temperature model: i) the average value of each phenological parameter at different temperatures, and ii) the average value of mean caterpillar abundance on each date throughout spring at different temperatures which depends on all phenological parameters. Both required marginalising random terms, but the method to do this differed.

(i) To estimate the height or width at different temperatures (Fig. 3c-d), half of the variance for each random term associated with each parameter was added to the estimate before exponentiating.

(ii) Since an analytical solution was not available, marginalisation was carried out by simulating from the posterior predictive distribution 10,000 times for each date:temperature combination and taking the average abundance. This allows visualisation of changes to the full phenological distribution with changing temperature (Fig. 4a). The duration was calculated for each temperature as the dates on which the average abundance exceeded the threshold (Fig. 4b), and the area was calculated as the sum of the average abundance across dates (Fig. 4c). Due to the uncertainty in the mean timing of the distribution the maximum average abundances reached are lower than those predicted from i).

907 **Appendix S5: Sliding window analysis**

908

909 Methods

910 We began our analyses by identifying the periods during which temperature best predicted the
911 thermal sensitivity of the mean timing, height and width parameters of the caterpillar
912 phenological distribution. As it is feasible that the most influential period could differ for each
913 parameter, we used a sliding window approach which allowed such. Therefore, as the number
914 of windows to consider was the product of the number of windows considered for each
915 parameter, for efficiency we applied a frequentist meta-analytic approach (using the metafor
916 package (Viechtbauer 2010)) to the site by year estimates for the three parameters. This allowed
917 us to compare sliding windows based on AIC.

918

919 Site by year model: To obtain estimates of the three phenological parameters for each site in
920 each year we modelled the phenological distribution of at each site in each year using the same
921 model composition as the spatiotemporal temperature model using RStan (Stan Development
922 Team 2020), but excluding the temperature fixed effects. From the model output the intercept
923 and random intercepts for each site, year and site by year combination could be summed to
924 obtain the estimate of each phenological parameter for each site in each year. The posterior
925 mode (calculated using the posterior.mode function in the MCMCglmm package (Hadfield
926 2010)) was used as our estimate of mean timing, height and width for each site by year
927 combination for the response variable in metafor (Viechtbauer 2010) multivariate meta-
928 analyses. The variance-covariance matrix of the posterior distributions for the three parameters
929 in each site in each year were included as the sampling variance.

930

We modelled the effect of temperature on each distribution parameter under a sliding window framework, allowing each parameter to be predicted by different time windows of temperature. For mean timing the window start dates ranged from day 58 to day 100, shifting in 7 day increments. For the height and width the window start dates ranged from 58 to 128, shifting in 14 day increments. The incremental shifts in start date were slightly higher resolution and restricted to an earlier period of the year for the mean timing parameter due to stronger a priori predictions from previous studies (Visser *et al.* 2006); whereas much less is known about the time windows that best predict the distribution height and width (see Visser *et al*. 2006) so we allowed larger increments to reduce the extent of multiple testing. All three parameters had windows ranging in duration from 28 to 98 days, increasing in duration in 14 day increments. This produced 30 window options for the mean timing variable and 21 for the height and width, resulting in 13231 models in total.

The metafor multivariate models included independent intercepts and temperature slopes for each of the response variable, as well as including year and each site in each year (site-year) as random terms for each response. As it is only possible to include two random terms that are independent for each response variable in the metafor package we selected year and site-year but not site. Random terms were estimated using an unstructured variance-covariance matrix. The models were fitted using maximum-likelihood rather than restricted maximum-likelihood to enable model comparison using AIC.

Supplementary results

Table S1: Window combinations for the models that did not converge in a sliding window analysis which allowed different temperature periods to predict the three parameters that describe the phenological distribution of caterpillar abundance. Shows the start date and duration of each window.

Mean Timing		**Height**		**Width**	
Start	Duration	Start	Duration	Start	Duration
93	28	72	70	100	28
93	28	72	84	100	28
93	28	58	98	100	28
100	56	72	70	128	28
100	56	72	70	114	42
100	56	72	84	128	28
100	56	58	98	128	28

Of the 13231 models run, 7 did not converge, the details of which can be found in Table S1.

As seen in Fig S1, all models with AIC's within 2 of the best fitting model for the mean timing and height parameters included the windows that were also in the best fitting model, however for the width parameter the windows used in models within 2 AICs of the best fitting were more varied, suggesting there is no particular time period between mid-Feb and late June during which temperature predicts the change in peak shape to a much greater extent (Fig. S3).

As the aim of this work was to identify the effect of spring temperatures on each metric of the caterpillar peak and not to identify the most influential time period of temperature throughout the year we proceeded using the windows of temperature identified in the best fitting model despite the lack of a clear optimal window for estimating the width parameter.

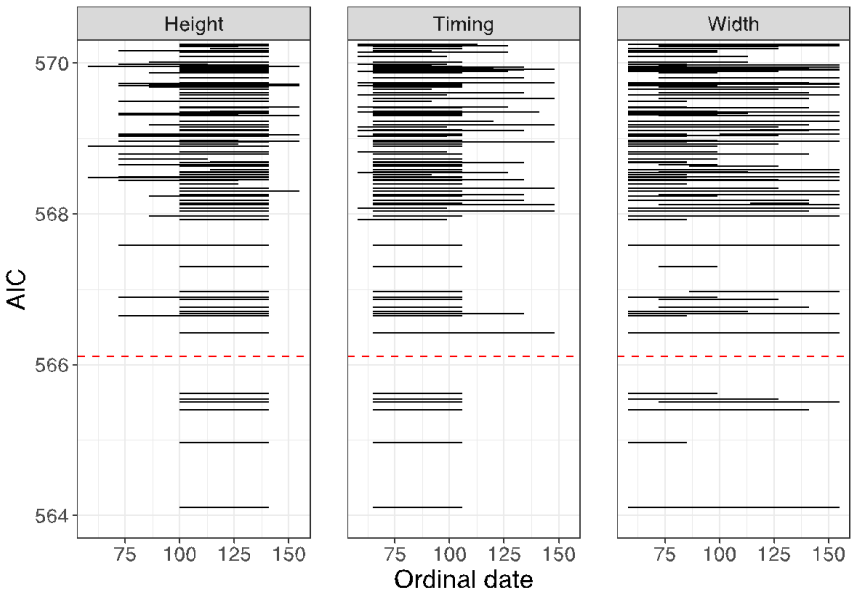

Figure S2: Plot of the AICs from models using different windows of temperature (horizontal black lines) as predictors of the three parameters describing the phenological distribution of caterpillar abundance. All lines beneath the red dashed line are within two AICs of the model with the lowest AIC value. Cropped Y axis, only showing subset of models with lower AICs.

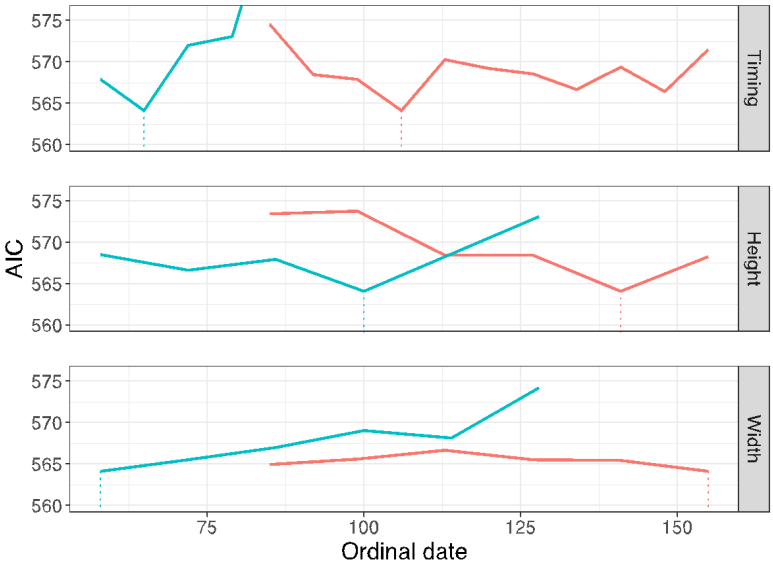

Figure S3: Plots of the minimum AIC from models using windows of temperature starting (blue) or ending (red) on each date for each parameter describing the phenological distribution of caterpillar abundance. Dashed vertical lines indicate the start and end dates with the lowest AICs.

Temperature mean, standard deviation and range in the identified windows:

The mean temperature during the mean timing parameter window was 5.83ºC, ranging from -3.05 to 3.06ºC with a standard deviation (sd) of 1.22 after mean centring (spatial: -1.73 - 1.48ºC; temporal: -2.13 - 1.57ºC). The mean temperature during the width parameter window was 7.81ºC , ranging from -2.50 to 2.17ºC with a sd of 0.85 after mean centring (spatial: -1.58 - 1.16ºC; temporal: -1.15 - 1.18ºC). The mean temperature during the height parameter window was 8.92ºC, ranging from -3.55 to 2.43ºC with a sd of 1.20 after mean centring (spatial: -1.59 - 1.05ºC; temporal: -2.40 - 2.01ºC).

Correlation among temperatures in identified windows:

The temperatures that contribute to each of the three best windows (one for timing, height and width) are overlapping (Figure 3a, Table S1). Therefore one would expect the effect of a change

in temperature to lead to a somewhat correlated response. When we estimate the pairwise correlations in temperatures between windows, we find that in space the correlations are very high (Table S2), whereas in time the correlation is weaker and there is no temporal correlation between the temperatures that predict timing and height. The stronger correlations between different windows in space (across sites) versus time (across years) is consistent with information about the position of the sliding windows stemming mainly from the temporal replication in the data (Shutt *et al.* 2019b).

Table S2: Comparison of the best windows identified for each pair of parameters (timing, height and width). Proportional overlap is the number of days that intersect divided by the summed number of days. Temperature correlations capture the correlation between the average temperatures obtained for pairs of parameters and is partitioned into spatiotemporal (using site-year mean temperatures), spatial (using site means) and temporal (using annual deviations from site means) estimates.

Parameter pairs	**Prop. overlap**	**Spatiotemporal cor.**	**Spatial cor.**	**Temporal cor.**
MeanTiming:Height	0.08	0.31	0.94	-0.06
MeanTiming:Width	0.3	0.78	0.98	0.58
Height:Width	0.3	0.79	0.99	0.71

Appendix S6: Site, year and site-year variance in models

The variance in timing, height and width that is distributed among site, year and site-year quantify are captured by random terms in the model, and all terms are significantly removed from 0 (Table S3).

Table S3: Posterior mode (95% credible intervals) for the variance attributed to the site, year and site-year (each site in each year) random terms for the timing, height and width parameters of the phenological distribution of caterpillars. Outlined for two models: the main spatiotemporal temperature model and the equivalent model that excludes the fixed effect temperature slopes for each parameter. As estimates are directly from the model the width and height terms are on the log-scale and the timing and width terms are scaled (original sd = 14.1)

	Random term	Spatiotemporal temperature model	Site by year model
Timing	Site	0.043 (0.025 - 0.096)	0.145 (0.085 - 0.254)
	Year	0.142 (0.089 - 1.033)	0.119 (0.06 - 0.782)
	Site-year	0.012 (0.006 - 0.031)	0.019 (0.01 - 0.042)
Height	Site	0.744 (0.516 - 1.333)	0.860 (0.559 - 1.415)
	Year	0.134 (0.028 - 1.267)	0.397 (0.216 - 3.123)
	Site-year	0.459 (0.369 - 0.636)	0.462 (0.354 - 0.611)
Width	Site	0.029 (0.011 - 0.066)	0.029 (0.014 - 0.076)
	Year	0.055 (0.021 - 0.508)	0.020 (0.01 - 0.258)
	Site-year	0.034 (0.018 - 0.065)	0.037 (0.016 - 0.066)

In the site by year model (i.e. a model without temperature predictors) we find substantial variation in timing among sites and years. When temperature is included in the model this leads to a substantial reduction (-70%) in the among site variance (Table S3). The variation in height is greatest among sites, but also substantial among years and site-years and this variance is substantially reduced among years when temperature is included in the model (though credible intervals are broad). An implication of the substantial site-year variance is that the height of the caterpillar guild abundance peak may be quite idiosyncratic in space and time and not solely predictable on the basis of temperature. For the width parameter the main difference seen was an increased variance among years when the temperature slope was included, supporting our finding from the space vs time model that temporal temperature variation does not predict the width of the phenological distribution.

Appendix S7: Issues with a Poisson GLMM approach to modelling temperature effects

The non-linear Gaussian function used by our study has more often been modelled as the re-parameterised linear form in a Poisson GLMM (Eq. S8).

Eq. S8: $$y = \beta_0 + \beta_1 d + \beta_2 d^2$$

Previous work has suggested that by extending Eq. S8 to include an interaction between a temperature variable and the date parameter, d (Eq. S9) it is possible to estimate the change in mean timing with temperature (Chevin *et al.* 2015; Edwards & Crone 2021).

Eq. S9: $$y = \beta_0 + \beta_1 d + \beta_2 d^2 + \beta_3 t + \beta_4 dt$$

The maximum height (H) of the distribution is reached at the mean timing (M), which can be simplified to $A + Bt$ (Eq. S10) where $A = -\frac{\beta_1}{2\beta_2}$ and B=$-\frac{\beta_4}{2\beta_2}$.

Eq. S10: $$M = -\frac{(\beta_1 + \beta_4 t)}{2\beta_2}$$

$$= -\frac{\beta_1}{2\beta_2} - \frac{\beta_4}{2\beta_2} t$$

$$= A + Bt$$

When quantifying the height of the phenological distribution ($d = M$) in Eq. S9, we found the model forces the height to be a quadratic function of temperature (Eq. S11).

Eq. S11: $$H = \beta_0 + \beta_1(A + Bt) + \beta_2(A + Bt)^2 + \beta_3 t + \beta_4(A + Bt)t$$

$$= \beta_0 + \beta_1 A + \beta_1 Bt + \beta_2 A^2 + \beta_2 2ABt + \beta_2 B^2 t^2 + \beta_3 t + \beta_4 A + \beta_4 Bt^2$$

$$= \beta_0 + \beta_1 A + \beta_2 A^2 + \beta_4 A + (\beta_1 B + \beta_2 2AB + \beta_3)t + (\beta_2 B^2 + \beta_4 B)t^2$$

As our interest was modelling linear effects of temperature on mean timing, height and width of the phenological distribution, this linear model composition has undesired properties.